OPEN ACCESS
Fractals, Vol. 31, No. 2 (2023) 2340016 (18 pages)

DOI: 10.1142/S0218348X23400169

World Scientific
www.worldscientific.com



# COMPUTATIONAL PERFORMANCES OF MORLET WAVELET NEURAL NETWORK FOR SOLVING A NONLINEAR DYNAMIC BASED ON THE MATHEMATICAL MODEL OF THE AFFECTION OF LAYLA AND MAJNUN

ZULQURNAIN SABIR,[*,†,‡‡] DUMITRU BALEANU,[‡,§,¶,‖,§§,†††]
MUHAMMAD ASIF ZAHOOR RAJA,[**,¶¶,†††]
ALI S. ALSHOMRANI,[††,‖‖] and EVREN HINCAL[*,***]

[*]*Department of Mathematics*
*Near East University, Nicosia 99138, Cyprus*

[†]*Department of Computer Science and Mathematics*
*Lebanese American University, Beirut, Lebanon*

[‡]*Department of Mathematics*
*Cankaya University, Ankara, Turkey*

[§]*Institute of Space Sciences, Magurele, Romania*

[¶]*Department of Medical Research*
*China Medical University Hospital*
*China Medical University, Taichung, Taiwan*

[‖]*Near East University, Mathematics Research Center*
*Nicosia, 99138, North Cyprus, Mersin 10, Turkey*

[**]*Future Technology Research Center*
*National Yunlin University of Science and Technology*
*123 University Road, Section 3, Douliou*
*Yunlin 64002, Taiwan, R.O.C.*

[†††]Corresponding authors.

††Faculty of Science, Department Mathematics
King Abdulaziz University, Jeddah 21589, Saudi Arabia
‡‡zulqurnain.sabir@neu.edu.tr
§§dumitru@cankaya.edu.tr
¶¶rajamaz@yuntech.edu.tw
‖‖aszalshomrani@kau.edu.sa
***evren.hincal@neu.edu.tr

Received December 31, 2021
Accepted June 5, 2022
Published February 28, 2023



## Abstract

The aim of this study is to design a novel stochastic solver through the Morlet wavelet neural networks (MWNNs) for solving the mathematical Layla and Majnun (LM) system. The numerical representations of the mathematical LM system have been presented by using the MWNNs along with the optimization is performed through the hybridization of the global and local search schemes. The local active-set (AS) and global genetic algorithm (GA) operators have been used to optimize an error-based merit function using the differential LM model and its initial conditions. The correctness of the MWNNs using the local and global operators is observed through the comparison of the obtained solutions and the Adams scheme, which is used as a reference solution. For the stability of the MWNNs using the global and local operators, the statistical performances with different operators have been provided using the multiple executions to solve the nonlinear LM system.

*Keywords*: Layla and Majnun; Morlet Wavelet Neural Networks; Mathematical Model; Local and Global Operators; Statistical Analysis.

## Abbreviations

| | |
|---|---|
| MWNNs | Morlet wavelet neural networks |
| LM | Layla and Majnun |
| AS | Active-set |
| GAs | Genetic Algorithms |
| MWNNs-AS-GA | Hybrid of MWNNs with GAs and AS algorithms |
| TIC | Theil's inequality coefficient |
| SIR | semi- interquartile range |
| VAF | variance account for |
| AS-GAs | Hybrid of GAs with AS algorithms |
| ICs | Initial conditions |
| EVAF | Error in VAF |
| MAD | Mean absolute deviation |
| Min, Med, Max, SD | Minimum, Median, Maximum and Standard deviation |

## 1. INTRODUCTION

Physiology generally represents a quantitative study of consciousness, even though described by the American psychiatric organizations.[1–4] Such a small number of psychiatrists as well as mathematicians often will use mathematical structures to depict love relationships.[5–7] Humanity, social dimensions, life quality, cognition, including therapeutic practices are only a couple of minor comments section covered by this complex concept. What really is love? It is a basic query that arises inside the brain. Love is puzzling, to say the least, yet it may be frightening at times. Whenever anyone falls in love, human hearts bow down, while if there is nothing about love, entire earth appears to be revolving. Through understanding its environmental impacts and behavioral events that contribute also in inspiring humans thinking person began a relationship, the biological causes of certain

emotions are however revealed. Sassi Punnuh, Heer Ranjha, Romeo Julliet, Sohni Mahiwal, Lancelot Guinevere, and many other romantic stories abound in modern existence. This study shows a historical Layla and Majnun story. Majnun is known as a mad person in Persian and this name has got huge fame in the Arab region that is considered a basic area of Majnun. This realistic love story presents that a young Majnun intensely fell in love with Layla. He wanted to marry Laila and sent a proposal to her house. The proposal was denied by the Layla's father and he pressurized Layla emotionally and physiologically not to marry Majnun. This was a shocking news for Majnun and he started writing poems for Layla and wandering in the deserts. Layla also had same feelings of shock for Majnun and day by day she fell ill and finally died. Majnun passed the days and nights in the deserts and finally he too died in the desert.

The romantic relationship is defined in the form of the complex variables. The mathematical form of the system has two kinds of dynamics that are described with the time variation based on the romantic feelings of two humans using the complex variables of love and emotions. Subsequently, the complex variable values contain both magnitude and phase, they are capable to indicate more types of feeling. For example, the conflict of emotions can be apathy hate and the spirits of two humans can occur, if they have thoughts, feelings and emotions for one another, while the other things look useless. Love is the part of the soul without the prejudice of religion, color and creed. The feelings and emotions do not only occur in the humans, but these feelings have been there in birds, insects, animals and other living things. However, there are numerous complex system models that can be observed in various areas, like as the plasma physics,[8] high-energy accelerators,[9] optical systems,[10] rotor dynamics,[11] chaotic systems,[12] HIV/AIDS model,[13] a tumor-immune interaction model,[14] cancer model,[15] Buongiorno's model,[16] spherical strange attractor model,[17] TB and HIV co-infection model,[18] chaotic attractors,[19] COVID-19 model,[20] modeling of Gemini virus,[21] automatic voltage regulator system,[22] fractional order systems,[23] tumor-immune system,[24] COVID-19 model with transmission through infected environment,[25] HIV infection spread model,[26] stiff differential system in chemistry kinetics[27] and many other that can be seen in Refs. 28–33.

The purpose of this study is to provide the numerical performances of an affection story of Layla and Majnun (LM) mathematical model using the MWNNs along with the optimization performances through the hybridization of the global and local search schemes. The MWNNs applied together with the local active-set (AS) and global genetic algorithm (GA) operators, i.e. MWNNs-AS-GA to solve the differential LM mathematical model.

This paper is arranged as follows. The general form of the LM is provided in Sec. 2. The novel features and summary of the stochastic operators are provided in Sec. 3. The methodology-based MWNNs-AS-GA is designed in Sec. 4. The simulations of the LM mathematical model are presented in Sec. 5 and the conclusion is reported in Sec. 6.

## 2. NONLINEAR FORM OF LM MATHEMATICAL MODEL

The present representations are related to present the nonlinear form of the LM mathematical model. However, these arbitrarily complex relationships indicate the degrees of freedom. The nonlinear form using the two complex variables together with four parameters is provided as[34,35]

$$\begin{cases} \dfrac{dM(y)}{dy} = L^2(y) + \beta_c M(y) + \beta_a, \quad M_0 = k_1, \\ \dfrac{dL(y)}{dy} = M^2(y) + \beta_d L(y) + \beta_b, \quad L_0 = k_2. \end{cases} \tag{1}$$

Here $\beta_d < 0$, $\beta_b < 0$, $\beta_c < 0$ and $\beta_a < 0$, $k_1$ and $k_2$ are the initial conditions, the variables $M(y)$ and $L(y)$ represent the feelings of Majnun and Layla for each other. $\beta_b$ and $\beta_a$ are the constant parameters that represents the feeling impacts based on the environment. $\beta_b < 0$ is the unkindness attitude of society and Layla family. The fixed $\beta_a > 0$ value shows the sympathy effects for Majnun. Consequently, the environmental impacts indicate the hope for Majnun. The parameters $M^2(y)$ and $L^2(y)$ represent the factors of extreme love and any sign of gentleness from the other stimulated them generally. The true love indication has been achieved by taking the fixed values of $\beta_c < 0$ and $\beta_d < 0$. The system (1) is extended by taking $M = M_r + iM_i$

and $L = L_r + iL_i$, written as

$$\begin{cases} \dfrac{dM_r(y)}{dy} = L_r^2(y) - L_i^2(y) + \beta_a + \beta_c M_r(y), \\ \dfrac{dM_i(y)}{dy} = -2L_r(y)L_i(y) + \beta_c M_i(y), \\ \dfrac{dL_r(y)}{dy} = M_r^2(y) - M_i^2(y) + \beta_b + \beta_d L_r(y), \\ \dfrac{dL_i(y)}{dy} = 2M_r(y)M_i(y) + \beta_d L_i(y), \\ M_r(0) = k_1, \quad M_i(0) = k_2, \\ L_r(0) = k_3, \quad L_i(0) = k_4, \end{cases} \tag{2}$$

Here, Majnun's imaginary and real feelings are $M_i(y)$ and $M_r(y)$. While Layla's imaginary and real feelings are $L_i(y)$ and $L_r(y)$.

## 3. NOVEL FEATURES AND STOCHASTIC SOLVERS APPLICATIONS

The stochastic computing solvers through the MWNNs-AS-GA operators have been used to solve the LM mathematical system. The MWNNs-AS-GA solver has never been applied before to solve the LM nonlinear mathematical system. The stochastic solvers using the heuristic, swarming along with the local search algorithms have been used to solve a number of singular, nonlinear, stiff and complex models.[36–50] Few novel features of this study are presented as

- The design of Morlet wavelet NNs is presented to solve the romantic LM mathematical system.
- The numerical solutions of the romantic LM mathematical system are successfully presented by using the proposed MWNN along with the optimization procedures of AS and GA approaches.
- The overlapping of the calculated and the reference solutions indorses the exactness of the designed MWNNs-AS-GA solver.
- The close values of the absolute error (AE) are performed to indorse the correctness of the designed MWNNs-AS-GA solver.
- The reliability of the MWNNs-AS-GA solver is observed by providing the statistical performances using different operators like TIC, SIR and VAF for solving the romantic LM mathematical system.

## 4. DESIGN PROCEDURES

This section provides the designed Morlet wavelet NNs structure by using the optimization procedures of the AS-GA to solve the romantic LM mathematical system. The procedural steps are divided in two steps to solve the romantic LM system as

- For the MWNNs parameters, a merit function is constructed using the differential romantic LM mathematical system and ICs.
- Essential backgrounds are provided in order to optimize the merit function using the AS-GA.

### 4.1. MWNNs Structure

The mathematical illustrations to solve the romantic LM mathematical system are presented to explore the MWNN-AS-GA operators. The proposed descriptions of the romantic LM mathematical system are signified as $\hat{M}_r$, $\hat{M}_i$, $\hat{L}_r$ and $\hat{L}_i$, given as

$$\begin{bmatrix} \hat{M}_r(y) \\ \hat{M}_i(y) \\ \hat{L}_r(y) \\ \hat{L}_i(y) \end{bmatrix} = \begin{bmatrix} \sum_{j=1}^{m} a_{M_r,j} q(w_{M_r,j} y + p_{M_r,j}), \\ \sum_{j=1}^{m} a_{M_i,j} q(w_{M_i,j} y + p_{M_i,j}), \\ \sum_{j=1}^{m} a_{L_r,j} q(w_{L_r,j} y + p_{L_r,j}), \\ \sum_{j=1}^{m} a_{L_i,j} q(w_{L_i,j} y + p_{L_i,j}) \end{bmatrix},$$

$$\begin{bmatrix} \hat{M}'_r(y), \\ \hat{M}'_i(y), \\ \hat{L}'_r(y), \\ \hat{L}'_i(y) \end{bmatrix} = \begin{bmatrix} \sum_{j=1}^{m} a_{M_r,j} q'(w_{M_r,j} y + p_{M_r,j}), \\ \sum_{j=1}^{m} a_{M_i,j} q'(w_{M_i,j} y + p_{M_i,j}), \\ \sum_{j=1}^{m} a_{L_r,j} q'(w_{L_r,j} y + p_{L_r,j}), \\ \sum_{j=1}^{m} a_{L_i,j} q'(w_{L_i,j} y + p_{L_i,j}) \end{bmatrix}. \tag{3}$$

$W$ is an unknown weight vector in system (3), written as

$$W = [W_{M_r}, W_{M_i}, W_{L_r}, W_{L_i}]$$

for

$$W_{M_r} = [a_{M_r}, \omega_{M_r}, p_{M_r}],$$
$$W_{M_i} = [a_{M_i}, \omega_{M_i}, p_{M_i}],$$
$$W_{L_r} = [a_{L_r}, \omega_{L_r}, p_{L_r}]$$

and

$$W_{L_i} = [a_{L_i}, \omega_{L_i}, p_{L_i}],$$

where

$$a_{M_r} = [a_{M_r,1}, a_{M_r,2}, \ldots, a_{M_r,m}],$$
$$a_{M_i} = [a_{M_i,1}, a_{M_i,2}, \ldots, a_{M_i,m}],$$
$$a_{L_r} = [a_{L_r,1}, a_{L_r,2}, \ldots, a_{L_r,m}],$$
$$a_{L_i} = [a_{L_i,1}, a_{L_i,2}, \ldots, a_{L_i,m}],$$
$$w_{M_r} = [w_{M_r,1}, w_{M_r,2}, \ldots, w_{M_r,m}],$$
$$w_{M_i} = [w_{M_i,1}, w_{M_i,2}, \ldots, w_{M_i,m}],$$
$$w_{L_r} = [w_{L_r,1}, w_{L_r,2}, \ldots, w_{L_r,m}],$$
$$w_{L_i} = [w_{L_i,1}, w_{L_i,2}, \ldots, w_{L_i,m}],$$
$$p_{M_r} = [p_{M_r,1}, p_{M_r,2}, \ldots, p_{M_r,m}],$$
$$p_{M_i} = [p_{M_i,1}, p_{M_i,2}, \ldots, p_{M_i,m}],$$
$$p_{L_r} = [p_{L_r,1}, p_{L_r,2}, \ldots, p_{L_r,m}],$$
$$p_{L_i} = [p_{L_i,1}, p_{L_i,2}, \ldots, p_{L_i,m}].$$

The MWNNs along with the AS-GA have never been applied before to solve the romantic LM mathematical system. The mathematical form of MW function is provided as

$$q(y) = \cos(1.75y)\exp(-1.75y^2),$$

$$\begin{bmatrix} \hat{M}_r(y), \\ \hat{M}_i(y), \\ \hat{L}_r(y), \\ \hat{L}_i(y), \end{bmatrix}$$

$$= \begin{bmatrix} \sum_{i=1}^{m} a_{M_r,j}\cos(1.75(w_{M_r,j}y + p_{M_r,j}))\, e^{-0.5(w_{M_r,j}y+p_{M_r,j})^2}, \\ \sum_{i=1}^{m} a_{M_i,j}\cos(1.75(w_{M_i,j}y + p_{M_i,j}))\, e^{-0.5(w_{M_i,j}y+p_{M_i,j})^2}, \\ \sum_{i=1}^{m} a_{L_r,j}\cos(1.75(w_{L_r,j}y + p_{L_r,j}))\, e^{-0.5(w_{L_r,j}y+p_{L_r,j})^2}, \\ \sum_{i=1}^{m} a_{L_i,j}\cos(1.75(w_{L_i,j}y + p_{L_i,j}))\, e^{-0.5(w_{L_i,j}y+p_{L_i,j})^2} \end{bmatrix},$$

$$\begin{bmatrix} \hat{M}_r'(y), \\ \hat{M}_i'(y), \\ \hat{L}_r'(y), \\ \hat{L}_i'(y) \end{bmatrix}$$

$$= \frac{d}{dy}\begin{bmatrix} \sum_{i=1}^{m} a_{M_r,j}\cos(1.75(w_{M_r,j}y + p_{M_r,j}))\, e^{-0.5(w_{M_r,j}y+p_{M_r,j})^2}, \\ \sum_{i=1}^{m} a_{M_i,j}\cos(1.75(w_{M_i,j}y + p_{M_i,j}))\, e^{-0.5(w_{M_i,j}y+p_{M_i,j})^2}, \\ \sum_{i=1}^{m} a_{L_r,j}\cos(1.75(w_{L_r,j}y + p_{L_r,j}))\, e^{-0.5(w_{L_r,j}y+p_{L_r,j})^2}, \\ \sum_{i=1}^{m} a_{L_i,j}\cos(1.75(w_{L_i,j}y + p_{L_i,j}))\, e^{-0.5(w_{L_i,j}y+p_{L_i,j})^2} \end{bmatrix}. \quad (4)$$

A merit function is provided as

$$\sum_{\text{Fit}} = \sum_{1} + \sum_{2} + \sum_{3} + \sum_{4} + \sum_{5}, \quad (5)$$

$$\sum_{1} = \frac{1}{N}\sum_{j=1}^{N}\begin{bmatrix} (\hat{M}_r')_j - (\hat{L}_r^2)_j + (\hat{L}_i^2)_j \\ -\beta_a - \beta_c(\hat{M}_r)_j \end{bmatrix}^2, \quad (6)$$

$$\sum_{2} = \frac{1}{N}\sum_{j=1}^{N}\begin{bmatrix} (\hat{M}_i')_j + 2(\hat{L}_r)_j(\hat{L}_i)_j \\ -\beta_c(\hat{M}_i)_j \end{bmatrix}^2, \quad (7)$$

$$\sum_{3} = \frac{1}{N}\sum_{j=1}^{N}\begin{bmatrix} (\hat{L}_r')_j - (\hat{M}_r^2)_j + (\hat{M}_i^2)_j \\ -\beta_b - \beta_d(\hat{L}_r)_j \end{bmatrix}^2, \quad (8)$$

$$\sum_{4} = \frac{1}{N}\sum_{j=1}^{N}\begin{bmatrix} (\hat{L}_i')_j - 2(\hat{M}_r)_j(\hat{M}_i)_j \\ -\beta_d(\hat{L}_i)_j \end{bmatrix}^2, \quad (9)$$

$$\sum_{5} = \frac{1}{4}\begin{bmatrix} ((\hat{M}_r)_0 - k_1)^2 + ((\hat{M}_i)_0 - k_2)^2 \\ +((\hat{L}_r)_0 - k_3)^2 + ((\hat{L}_i)_0 - k_4)^2 \end{bmatrix}, \quad (10)$$

where $(\hat{M}_r)_j = M_r(y_j)$, $(\hat{M}_i)_j = M_i(y_j)$, $(\hat{L}_r)_j = L_r(y_j)$, $(\hat{L}_i)_j = L_i(y_j)$, $y_j = jh$ and $Nh = 1$. The values $\sum_1$, $\sum_2$, $\sum_3$ and $\sum_4$ are the values of the merit functions-based on the network (2), whereas $\sum_5$ represents the ICs of the LM mathematical system (2).

**Table 1 Optimization of the MWNNs-AS-GA to Solve the Mathematical LM Model.**

**Start of GA**

**Inputs**: Chromosomes: $W = [a, w, p]$

**Population**: Chromosomes set is given as

$$W = [W_{M_r}, W_{M_i}, W_{L_r}, W_{L_i}]$$

for

$$W_{M_r} = [a_{M_r}, \omega_{M_r}, p_{M_r}],$$
$$W_{L_r} = [a_{L_r}, \omega_{L_r}, p_{L_r}]$$

and

$$W_{L_i} = [a_{L_i}, \omega_{L_i}, p_{L_i}],$$

where

$a_{M_r} = [a_{M_r,1}, a_{M_r,2}, \ldots, a_{M_r,m}]$, $a_{M_i} = [a_{M_i,1}, a_{M_i,2}, \ldots, a_{M_i,m}]$, $a_{L_r} = [a_{L_r,1}, a_{L_r,2}, \ldots, a_{L_r,m}]$, $a_{L_i} = [a_{L_i,1}, a_{L_i,2}, \ldots, a_{L_i,m}]$, $w_{M_r} = [w_{M_r,1}, w_{M_r,2}, \ldots, w_{M_r,m}]$, $w_{M_i} = [w_{M_i,1}, w_{M_i,2}, \ldots, w_{M_i,m}]$, $w_{L_r} = [w_{L_r,1}, w_{L_r,2}, \ldots, w_{L_r,m}]$, $w_{L_i} = [w_{L_i,1}, w_{L_i,2}, \ldots, w_{L_i,m}]$, $p_{M_r} = [p_{M_r,1}, p_{M_r,2}, \ldots, p_{M_r,m}]$, $p_{M_i} = [p_{M_i,1}, p_{M_i,2}, \ldots, p_{M_i,m}]$, $p_{L_r} = [p_{L_r,1}, p_{L_r,2}, \ldots, p_{L_r,m}]$, $p_{L_i} = [p_{L_i,1}, p_{L_i,2}, \ldots, p_{L_i,m}]$.

**Outputs**: Global weights: $W_{\text{Best}-\text{GA}}$

**Initialization**: To select the chromosomes, adjust $W_{\text{Best}-\text{GA}}$

**Fit Assessment**: Modify $\sum_{\text{Fit}}$ in the population using Eqs. (5)–(10).

**Stopping standards**: The algorithms stop, if $\sum_{\text{Fit}} = 10^{-18}$, Generations = 130, TolCon = $10^{-19}$, StallLimit = 210, TolFun = $10^{-21}$, PopSize = 330.

Move to [storage]

**Ranking**: Adjust $W_{\text{Best}-\text{GA}}$ using the population for$\sum_{\text{Fit}}$.

**Storage**: Function count, $W_{\text{Best}-\text{GA}}$, time, $\sum_{\text{Fit}}$ and iterations.

**End of [GA]**

**Start AS**

**Inputs**: $W_{\text{Best}-\text{GA}}$.

**Output**: $W_{\text{GA}-\text{AS}}$ represents the GA-AS values.

**Initialize**: $W_{\text{Best}-\text{GA}}$, iterations and assignments.

**Stopping conditions**: Terminate if [$\sum_{\text{Fit}} = 10^{-19}$], [MaxFunEvals = 330000], [Iterations = 950], [TolX = TolFun = $10^{-22}$] and [TolCon = $10^{-18}$].

**Fitness valuation**: Calculate $\sum_{\text{Fit}}$ and W for Eqs. (5)–(10).

**Amendments**: Control fmincon for AS, compute $\sum_{\text{Fit}}$ for (5)–(10) systems

**Accumulate**: Transform $W_{\text{GA}-\text{AS}}$, $\sum_{\text{Fit}}$, function counts, time, iterations for AS trials.

**End of AS**

## 4.2. Optimization Performances

The optimization performances based on the AS-GA approach are provided in this section to solve the mathematical LM nonlinear model. The design of the MWNNs using the optimization performances of the AS-GA to solve the mathematical LM nonlinear model is tabulated in Table 1.

The global search GA operator is used as an optimization procedure for solving a class of mathematical LM model. The procedures based on GA have been implemented to solve various complex, stiff and nonlinear networks. For best system outputs, GA is executed by the selection, reproduction and crossover operators. GA has been used in various applications in recent years.[51–55] AS is a local search, rapid, optimization-based operator that can be applied for the constrained/unconstrained systems. AS is performed in numerous optimizations networks, like singular boundary value problems,[56] food chain models,[57] nonlinear problems with-monotone operators,[58] nonlinear singular heat conduction model[59] and mosquito dispersal model.[60] The hybridization of the AS-GA is applied to eliminate the sluggishness of the GA for solving the mathematical LM model.

## 4.3. Performance Measures

This section represents the statistical measures based on the TIC, VAF, mean absolute deviation

(MAD) and SIR together with its Global depictions of TIC and VAF for LM system given as

$$\begin{bmatrix}\mathrm{TIC}_{M_r}\\ \mathrm{TIC}_{M_i}\\ \mathrm{TIC}_{L_r}\\ \mathrm{TIC}_{L_i}\end{bmatrix} = \begin{bmatrix} \dfrac{\sqrt{\frac{1}{n}\sum_{j=1}^{n}\left((M_r)_j-(\hat{M}_r)_j\right)^2}}{(\sqrt{\frac{1}{n}\sum_{j=1}^{n}(M_r^2)_j}+\frac{1}{n}\sum_{j=1}^{n}(\hat{M}_r^2)_j)} \\ \dfrac{\sqrt{\frac{1}{n}\sum_{j=1}^{n}\left((M_i)_j-(\hat{M}_i)_j\right)^2}}{(\sqrt{\frac{1}{n}\sum_{j=1}^{n}(M_i^2)_j}+\frac{1}{n}\sum_{j=1}^{n}(\hat{M}_i^2)_j)} \\ \dfrac{\sqrt{\frac{1}{n}\sum_{j=1}^{n}\left((L_r)_j-(\hat{L}_r)_j\right)^2}}{(\sqrt{\frac{1}{n}\sum_{j=1}^{n}(L_r^2)_j}+\frac{1}{n}\sum_{j=1}^{n}(\hat{L}_r^2)_j)} \\ \dfrac{\sqrt{\frac{1}{n}\sum_{j=1}^{n}\left((L_i)_j-(\hat{L}_i)_j\right)^2}}{(\sqrt{\frac{1}{n}\sum_{j=1}^{n}(L_i^2)_j}+\frac{1}{n}\sum_{j=1}^{n}(\hat{L}_i^2)_j)} \end{bmatrix}, \tag{11}$$

$$\begin{cases} \begin{bmatrix}\mathrm{VAF}_{M_r}\\ \mathrm{VAF}_{M_i}\\ \mathrm{VAF}_{L_r}\\ \mathrm{VAF}_{L_i}\end{bmatrix} = \begin{bmatrix} \left(1-\frac{\mathrm{var}((M_r)_j-(\hat{M}_r)_j)}{\mathrm{var}(M_r)_j}\right)\times 100 \\ \left(1-\frac{\mathrm{var}((M_i)_j-(\hat{M}_i)_j)}{\mathrm{var}(M_i)_j}\right)\times 100 \\ \left(1-\frac{\mathrm{var}((L_r)_j-(\hat{L}_r)_j)}{\mathrm{var}(L_r)_j}\right)\times 100 \\ \left(1-\frac{\mathrm{var}((L_i)_j-(\hat{L}_i)_j)}{\mathrm{var}(L_i)}\right)\times 100 \end{bmatrix}, \\ \begin{bmatrix}\mathrm{EVAF}_{M_r}\\ \mathrm{EVAF}_{M_i}\\ \mathrm{EVAF}_{L_r}\\ \mathrm{EVAF}_{L_i}\end{bmatrix} = \begin{bmatrix} |100-\mathrm{VAF}_{M_r}| \\ |100-\mathrm{VAF}_{M_i}| \\ |100-\mathrm{VAF}_{L_r}| \\ |100-\mathrm{VAF}_{L_i}| \end{bmatrix}, \end{cases} \tag{12}$$

$$\begin{cases} \mathrm{SIR} = 0.5(Q_3-Q_1), \\ Q_1 \text{ and } Q_3 \text{ are the } 1^{\mathrm{st}} \text{ and } 3^{\mathrm{rd}} \text{ quartiles}, \end{cases}$$

$$\begin{bmatrix}\mathrm{MAD}_{M_r}\\ \mathrm{MAD}_{M_i}\\ \mathrm{MAD}_{L_r}\\ \mathrm{MAD}_{L_i}\end{bmatrix} = \begin{bmatrix} \sum_{j=1}^{n}|(M_r)_j-(\hat{M}_r)_j| \\ \sum_{j=1}^{n}|(M_i)_j-(\hat{M}_i)_j| \\ \sum_{j=1}^{n}|(L_r)_j-(\hat{L}_r)_j| \\ \sum_{j=1}^{n}|(L_i)_j-(\hat{L}_i)_j| \end{bmatrix}. \tag{13}$$

## 5. SIMULATIONS AND RESULTS

This section represents the simulations that have been performed for solving a mathematical LM model. The obtained outcomes have been compared with the reference results to perform the correctness of the mathematical LM model. The statistical illustrations using different performances have been drawn to validate the consistency of the MWNNs-AS-GA. The mathematical LM model by taking the literature values is given as

$$\begin{cases} \dfrac{dM_r(y)}{dy} = L_r^2(y)-L_i^2(y)-M_r(y)+1, \\ \dfrac{dM_i(y)}{dy} = -2L_r(y)L_i(y)-M_i(y), \\ \dfrac{dL_r(y)}{dy} = M_r^2(y)-M_i^2(y)-\beta_d L_r(y)-1, \\ \dfrac{dL_i(y)}{dy} = 2M_r(y)M_i(y)-L_i(y), \\ M_r(0)=0.2, M_i(0)=0.1, \\ L_r(0)=0.2, L_i(0)=0.1. \end{cases} \tag{14}$$

A merit function based on the mathematical LM model is shown as

$$\sum_{Fit} = \frac{1}{N}\sum_{j=1}^{N}\left(\begin{bmatrix}(\hat{M}_r')_j-(\hat{L}_r^2)_j+(\hat{L}_i^2)_j \\ +(\hat{M}_r)_j-1\end{bmatrix}^2 + \begin{bmatrix}(\hat{M}_i')_j+2(\hat{L}_r)_j(\hat{L}_i)_j \\ +(\hat{M}_i)_j\end{bmatrix}^2 + \begin{bmatrix}(\hat{L}_r')_j-(\hat{M}_r^2)_j+(\hat{M}_i^2)_j \\ +(\hat{L}_r)_j+1\end{bmatrix}^2 + \begin{bmatrix}(\hat{L}_i')_j-2(\hat{M}_r)_j(\hat{M}_i)_j \\ +(\hat{L}_i)_j\end{bmatrix}^2\right) + \frac{1}{4}\begin{bmatrix}((\hat{M}_r)_0-0.2)^2+((\hat{M}_i)_0-0.1)^2 \\ +((\hat{L}_r)_0-0.2)^2+((\hat{L}_i)_0-0.1)^2\end{bmatrix}. \tag{15}$$

For the numerical simulations of the mathematical LM system, the optimization is performed by using the AS-GA hybridization based on 30 executions. Ten neurons have been used throughout this study. The results-based best weights represent the proposed solutions of the mathematical LM model shown as

$$\hat{M}_r(y) = 0.7503\cos\left(\frac{7}{4}\begin{pmatrix}2.2018y \\ +3.1689\end{pmatrix}\right) \times e^{-0.5(2.2018y+3.1689)^2}$$

$$
\begin{aligned}
&- 0.1788\cos\left(\frac{7}{4}(0.1965y + 2.7419)\right)\\
&\times e^{-0.5(0.1965y+2.7419)^2}\\
&- 0.1322\cos\left(\frac{7}{4}(1.4451y + 3.6053)\right)\\
&\times e^{-0.5(1.4451y+3.6053)^2}\\
&+ 0.3294\cos\left(\frac{7}{4}(0.3405y - 0.6590)\right)\\
&\times e^{-0.5(0.3405y-0.6590)^2}\\
&+ 1.1904\cos\left(\frac{7}{4}(-1.462y - 2.5652)\right)\\
&\times e^{-0.5(-1.462y-2.5652)^2}\\
&- 0.4781\cos\left(\frac{7}{4}(-0.581y - 0.9040)\right)\\
&\times e^{-0.5(-0.581y-0.9040)^2}\\
&- 0.2852\cos\left(\frac{7}{4}(0.8042y + 1.5858)\right)\\
&\times e^{-0.5(0.8042y+1.5858)^2}\\
&+ 0.2496\cos\left(\frac{7}{4}(-0.411y + 0.6448)\right)\\
&\times e^{-0.5(-0.411y+0.6448)^2}\\
&+ 0.0112\cos\left(\frac{7}{4}(-0.333y + 0.2481)\right)\\
&\times e^{-0.5(-0.333y+0.2481)^2}\\
&+ 0.3852\cos\left(\frac{7}{4}(0.4117y - 1.1147)\right)\\
&\times e^{-0.5(0.4117y-1.1147)^2}, \qquad (16)\\
\hat{M}_i(y) = &-0.284\cos\begin{pmatrix}\frac{7}{4}(-0.672y\\ -1.4409)\end{pmatrix}\\
&\times e^{-0.5(-0.672y-1.440)^2}\\
&- 0.0098\cos\left(\frac{7}{4}(-1.925y - 1.3835)\right)\\
&\times e^{-0.5(-1.925y-1.3835)^2}\\
&- 1.7638\cos\left(\frac{7}{4}(0.0486y + 1.1166)\right)\\
&\times e^{-0.5(0.0486y+1.1166)^2}
\end{aligned}
$$

$$
\begin{aligned}
&- 0.1505\cos\left(\frac{7}{4}(-0.179y + 0.5979)\right)\\
&\times e^{-0.5(-0.179y+0.5979)^2}\\
&+ 0.1132\cos\left(\frac{7}{4}(0.8571y + 1.3848)\right)\\
&\times e^{-0.5(0.8571y+1.3848)^2}\\
&+ 1.1044\cos\left(\frac{7}{4}(-0.016y + 1.7525)\right)\\
&\times e^{-0.5(-0.016y+1.7525)^2}\\
&+ 0.5231\cos\left(\frac{7}{4}(-1.135y - 1.7680)\right)\\
&\times e^{-0.5(-1.135y-1.7680)^2}\\
&- 0.0026\cos\left(\frac{7}{4}(1.6598y + 1.2173)\right)\\
&\times e^{-0.5(1.6598y+1.2173)^2}\\
&- 0.8341\cos\left(\frac{7}{4}(-0.821y - 2.0612)\right)\\
&\times e^{-0.5(-0.821y-2.0612)^2}\\
&+ 0.0903\cos\left(\frac{7}{4}(1.0258y + 0.7932)\right)\\
&\times e^{-0.5(1.0258y+0.7932)^2}, \qquad (17)\\
\hat{L}_r(y) = &-0.815\cos\begin{pmatrix}\frac{7}{4}(-0.112y\\ -1.4561)\end{pmatrix}\\
&\times e^{-0.5(-0.112y-1.4561)^2}\\
&+ 0.5518\cos\left(\frac{7}{4}(-0.805y - 0.9453)\right)\\
&\times e^{-0.5(-0.805y-0.9453)^2}\\
&- 0.0398\cos\left(\frac{7}{4}(-0.125y - 1.9254)\right)\\
&\times e^{-0.5(-0.125y-1.9254)^2}\\
&- 0.1856\cos\left(\frac{7}{4}(0.6934y + 1.8404)\right)\\
&\times e^{-0.5(0.6934y+1.8404)^2}\\
&+ 0.1194\cos\left(\frac{7}{4}(1.6599y + 1.7872)\right)\\
&\times e^{-0.5(1.6599y+1.7872)^2}
\end{aligned}
$$

$$
\begin{aligned}
&- 0.0531\cos\left(\frac{7}{4}(1.3726y + 0.2681)\right)\\
&\times e^{-0.5(1.3726y+0.2681)^2}\\
&+ 0.6788\cos\left(\frac{7}{4}(1.9080y + 3.8806)\right)\\
&\times e^{-0.5(1.9080y+3.8806)^2}\\
&- 1.8736\cos\left(\frac{7}{4}(0.1363y + 2.1630)\right)\\
&\times e^{-0.5(0.1363y+2.1630)^2}\\
&+ 0.5372\cos\left(\frac{7}{4}(0.6214y + 0.8007)\right)\\
&\times e^{-0.5(0.6214y+0.8007)^2}\\
&- 0.4528\cos\left(\frac{7}{4}(-0.382y + 0.6039)\right)\\
&\times e^{-0.5(-0.382y+0.6039)^2}, \qquad (18)
\end{aligned}
$$

$$
\begin{aligned}
\hat{L}_i(y) = {} & 0.3547\cos\left(\frac{7}{4}(-1.521y\right.\\
&\left.-2.4021)\right)\\
&\times e^{-0.5(-1.521y-2.4021)^2}\\
&+ 0.2694\cos\left(\frac{7}{4}(-0.050y + 1.0070)\right)\\
&\times e^{-0.5(-0.050y+1.0070)^2}\\
&+ 0.2150\cos\left(\frac{7}{4}(1.3529y + 1.3685)\right)\\
&\times e^{-0.5(1.3529y+1.3685)^2}\\
&- 0.2153\cos\left(\frac{7}{4}(1.0161y + 1.5049)\right)\\
&\times e^{-0.5(1.0161y+1.5049)^2}\\
&+ 0.4593\cos\left(\frac{7}{4}(-1.098y - 2.522)\right)\\
&\times e^{-0.5(-1.098y-2.522)^2}\\
&- 0.6099\cos\left(\frac{7}{4}(-1.074y - 2.038)\right)\\
&\times e^{-0.5(-1.074y-2.038)^2}\\
&- 0.3806\cos\left(\frac{7}{4}(0.0503y - 1.3022)\right)\\
&\times e^{-0.5(0.0503y-1.3022)^2}\\
&- 1.7116\cos\left(\frac{7}{4}(0.4646y + 2.8207)\right)\\
&\times e^{-0.5(0.4646y+2.8207)^2}\\
&+ 0.1317\cos\left(\frac{7}{4}(-1.671y - 1.8833)\right)\\
&\times e^{-0.5(-1.671y-1.8833)^2}\\
&- 0.0642\cos\left(\frac{7}{4}(0.1944y - 2.4880)\right)\\
&\times e^{-0.5(0.1944y-2.4880)^2}. \qquad (19)
\end{aligned}
$$

The optimization of $\sum_{\text{Fit}}$ is performed through AS-GA using Eq. (5) to solve the mathematical LM system. The numerical values used in the above results (17)–(20) with 0.05 step size in the interval 0 and 1 to solve the mathematical LM system are plotted in the form of the best weights in Figs. 1a–1d. While, the mean, best and reference form of the results is plotted in Figs. 1e–1h to solve the mathematical LM system. These precise results overlapping indicate the correctness of the proposed MWNNs-AS-GA scheme. Figure 2 represents the plots of AE based best and mean values for solving the mathematical LM system. It is observed that the best AE performances for $M_r(y), M_i(y), L_r(y)$ and $L_i(y)$, are calculated as $10^{-6} - 10^{-9}, 10^{-6} - 10^{-8}, 10^{-6} - 10^{-9}$ and $10^{-6} - 10^{-8}$. However, the mean AE performances for $M_r(y), M_i(y), L_r(y)$ and $L_i(y)$ are calculated as $10^{-1} - 10^{-2}, 10^{-2} - 10^{-4}, 10^{-2} - 10^{-3}$ and $10^{-4} - 10^{-4}$.

Figure 3 provides the performance plots based EVAF and TIC operators to solve the mathematical LM system. In addition, the performances of MAD are also provided. The ideal outputs of $M_r(y)$ using the TIC and EVAF operators along with the MAD performances are calculated as $10^{-10} - 10^{-11}, 10^{-11} - 10^{-12}$ and $10^{-6} - 10^{-8}$. The ideal $M_i(y)$ outputs using the TIC, EVAF and MAD performances are calculated as $10^{-10} - 10^{-12}, 10^{-11} - 10^{-12}$ and $10^{-7} - 10^{-8}$. The ideal $L_r(y)$ outputs using the EVAF, TIC and MAD performances are calculated as $10^{-10} - 10^{-11}, 10^{-11} - 10^{-12}$ and $10^{-7} - 10^{-8}$. Likewise, the ideal $L_i(y)$ outputs using the EVAF, TIC and MAD performances are $10^{-10} - 10^{-12}, 10^{-9} - 10^{-10}$ and $10^{-7} - 10^{-8}$. It is concluded through these performance plots that the proposed MWNNs-AS-GA solver is an accurate and precise.

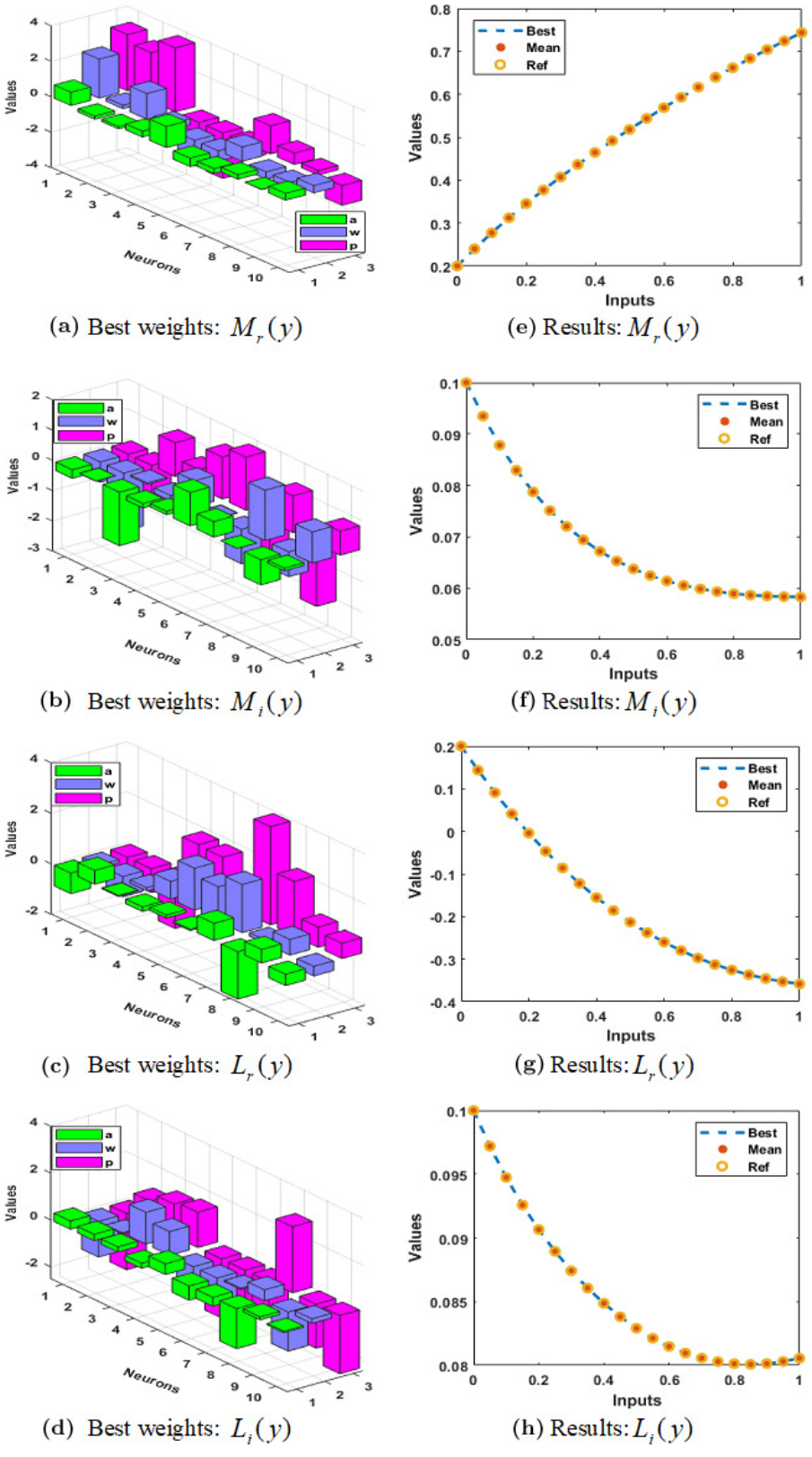


**Fig. 1** Comparison of results and best weights to solve the mathematical LM system.

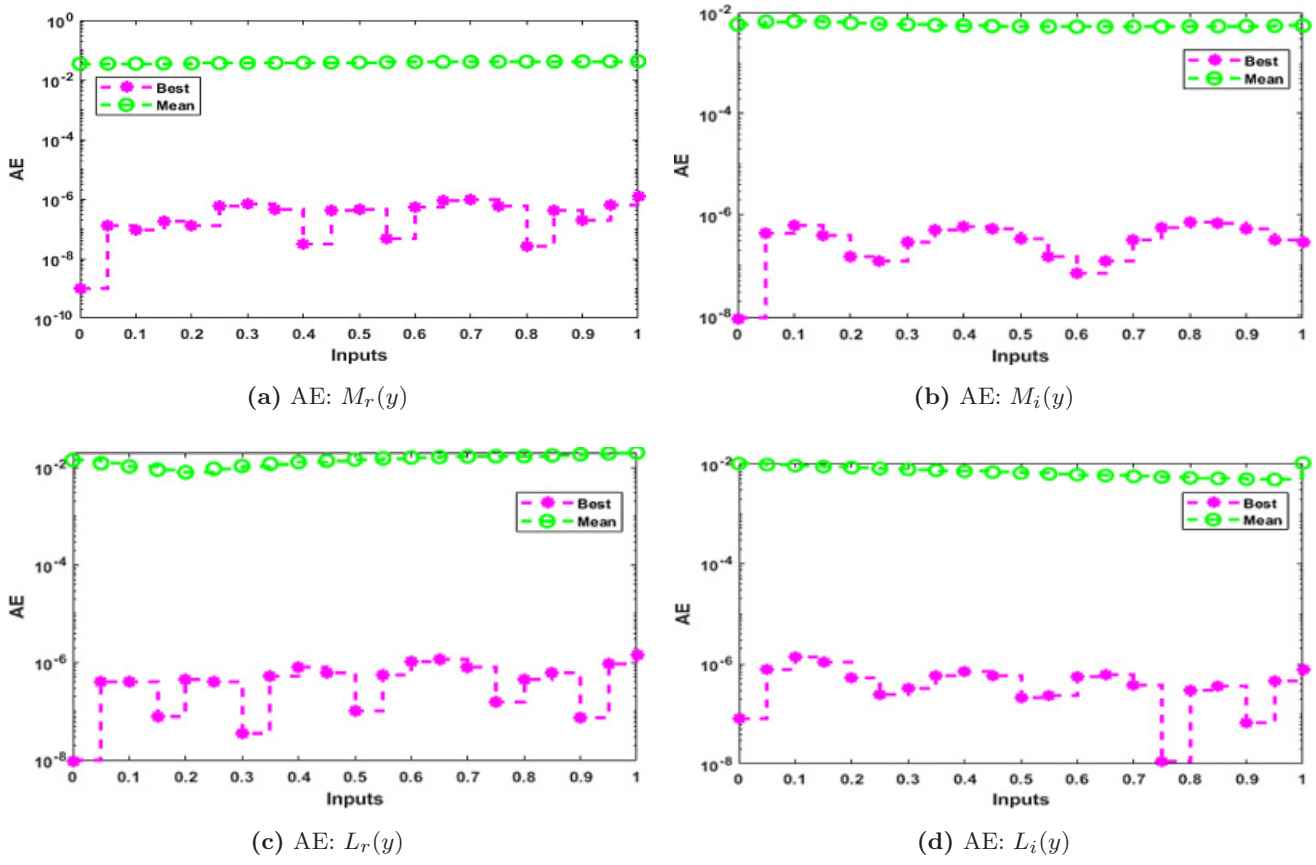


**(a)** AE: $M_r(y)$ **(b)** AE: $M_i(y)$

**(c)** AE: $L_r(y)$ **(d)** AE: $L_i(y)$

**Fig. 2** Comparison of results and best weights to solve the mathematical LM system.

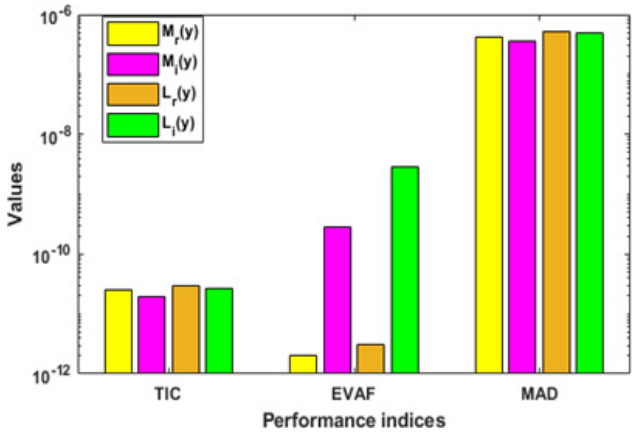


**Fig. 3** Comparison of results and best weights to solve the mathematical LM system.

The boxplots/histograms along with the statistical representations are provided in Figs. 4 and 5 to authenticate the convergence for the mathematical LM system. The TIC performances are presented in Fig. 4 for 30 runs to solve the mathematical LM system and a higher level of accuracy is achieved. The EVAF performances are drawn in Fig. 5, which represent a higher level of correctness. The achieved EVAF and TIC operator values using MWNNs-AS-GA are accurate to solve the mathematical LM system.

The statistical Minimum (Min), Mean, Maximum (Max), standard deviation (SD), SIR and Median (Med) plots are provided in Tables 2–5 to validate the mathematical LM model. The ideal presentations are provided in Min operators, while the worst values are described in Max values. For $M_r(y)$ class, the Min, Med, Max, S.I.R, SD and Mean measures lie $10^{-7}-10^{-10}, 10^{-6}-10^{-7}, 10^{-1}-10^{-2}, 10^{-6}-10^{-7}, 10^{-1}-10^{-2}$ and $10^{-2}-10^{-4}$. For $M_i(y)$, the Min, Med, Max, S.I.R, SD and Mean measures lie $10^{-7}-10^{-9}, 10^{-6}-10^{-7}, 10^{-2}-10^{-3}, 10^{-6}-10^{-7}, 10^{-2}-10^{-3}$ and $10^{-3}-10^{-4}$. Similarly, for $L_r(y)$, the Min, Med, Max, S.I.R, SD and Mean measures lie $10^{-7}-10^{-10}, 10^{-6}-10^{-7}, 10^{-1}-10^{-2}, 10^{-6}-10^{-7}, 10^{-2}-10^{-3}$ and $10^{-2}-10^{-4}$. For $L_i(y)$, the Min, Med, Max, S.I.R, SD and Mean measures lie $10^{-7}-10^{-9}, 10^{-6}-10^{-7}, 10^{-1}-10^{-2}, 10^{-6}-10^{-8}, 10^{-2}-10^{-3}$ and $10^{-3}-10^{-04}$. These small values represent the MWNNs-AS-GA

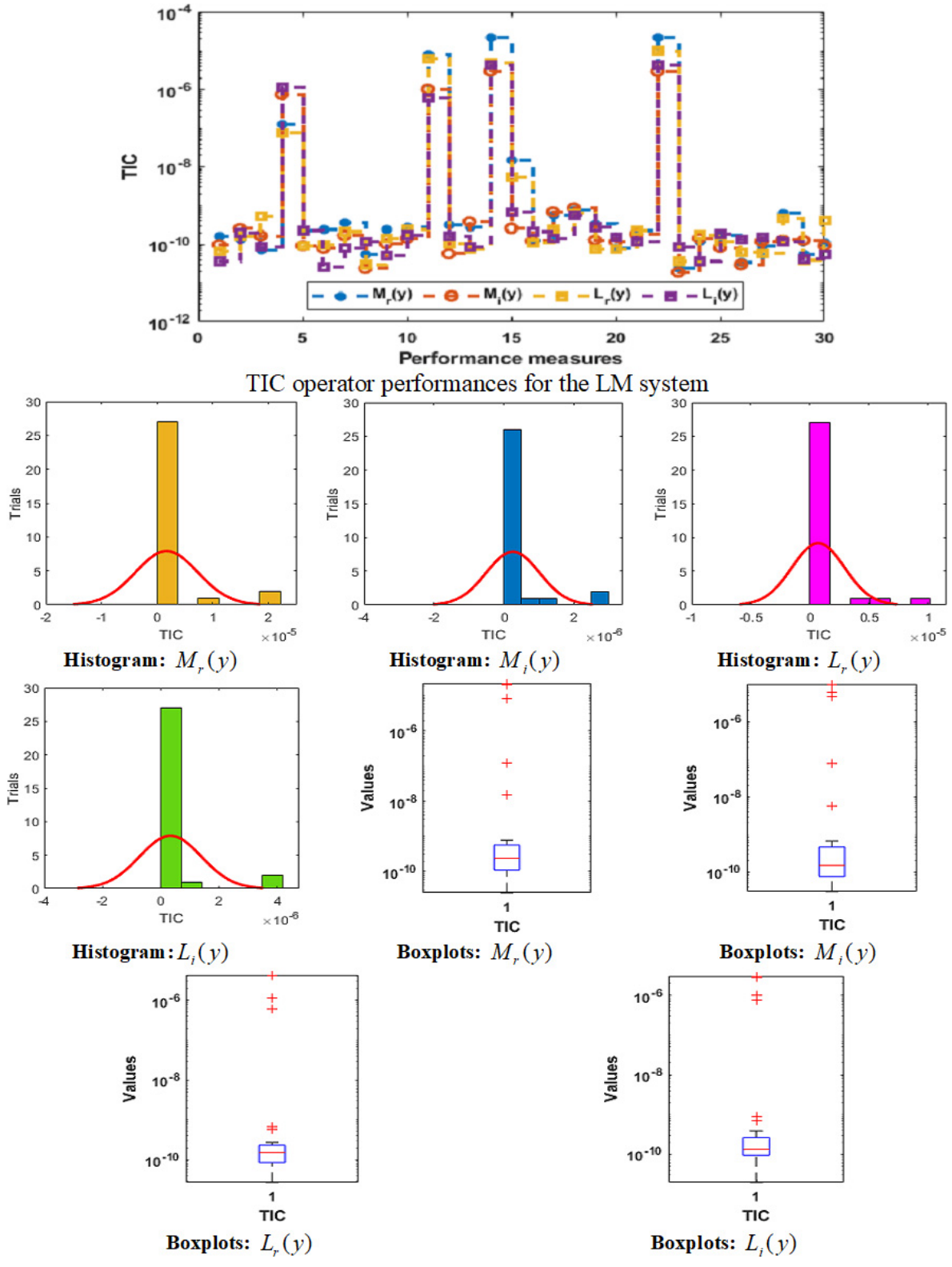


**Fig. 4** Comparison of results and best weights to solve the mathematical LM system.

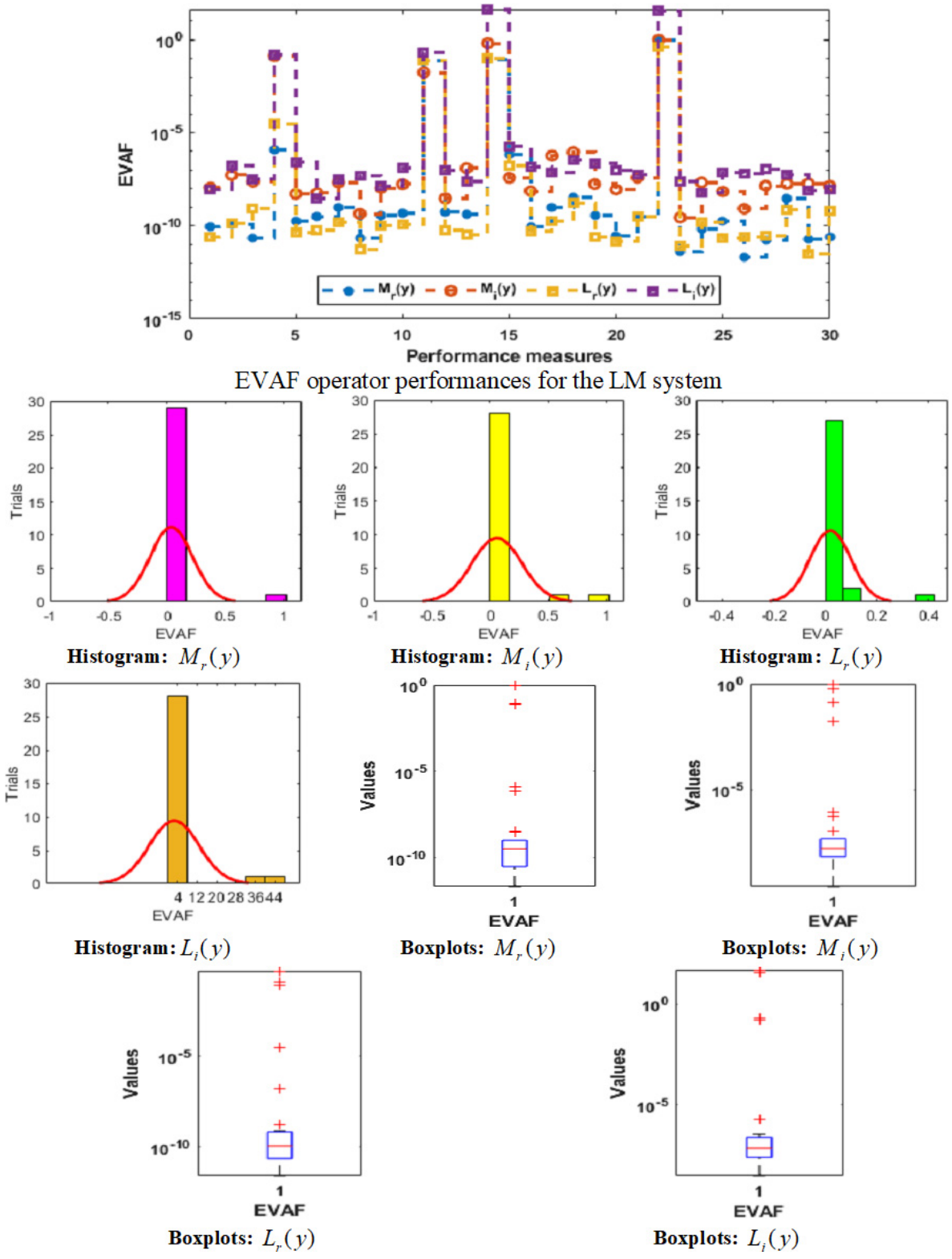


**Fig. 5** Comparison of results and best weights to solve the mathematical LM system.

**Table 2 Numerical Performance for the LM System-Based $M_r(y)$ Class.**

| $y$ | Min | Med | Max | SIR | STD | Mean |
|---|---|---|---|---|---|---|
| 0 | 2.574E−10 | 2.803E−07 | 5.832E−01 | 4.752E−07 | 1.183E−01 | 3.445E−02 |
| 0.05 | 1.301E−07 | 4.087E−06 | 5.578E−01 | 4.208E−06 | 1.159E−01 | 3.461E−02 |
| 0.1 | 9.565E−08 | 8.679E−06 | 5.351E−01 | 5.981E−06 | 1.144E−01 | 3.481E−02 |
| 0.15 | 1.802E−07 | 8.689E−06 | 5.151E−01 | 7.774E−06 | 1.137E−01 | 3.507E−02 |
| 0.2 | 1.332E−07 | 5.269E−06 | 4.979E−01 | 5.388E−06 | 1.138E−01 | 3.537E−02 |
| 0.25 | 3.423E−07 | 3.333E−06 | 4.834E−01 | 3.386E−06 | 1.146E−01 | 3.573E−02 |
| 0.3 | 2.881E−07 | 2.314E−06 | 4.714E−01 | 1.817E−06 | 1.159E−01 | 3.613E−02 |
| 0.35 | 6.563E−08 | 2.933E−06 | 4.619E−01 | 3.054E−06 | 1.177E−01 | 3.658E−02 |
| 0.4 | 3.133E−08 | 3.760E−06 | 4.644E−01 | 4.035E−06 | 1.199E−01 | 3.706E−02 |
| 0.45 | 2.177E−08 | 5.411E−06 | 4.916E−01 | 4.341E−06 | 1.224E−01 | 3.756E−02 |
| 0.5 | 7.212E−08 | 5.780E−06 | 5.180E−01 | 4.388E−06 | 1.250E−01 | 3.806E−02 |
| 0.55 | 4.588E−08 | 5.337E−06 | 5.437E−01 | 5.733E−06 | 1.278E−01 | 3.856E−02 |
| 0.6 | 1.289E−07 | 3.573E−06 | 5.687E−01 | 5.176E−06 | 1.306E−01 | 3.903E−02 |
| 0.65 | 4.167E−08 | 3.248E−06 | 5.930E−01 | 3.817E−06 | 1.335E−01 | 3.946E−02 |
| 0.7 | 1.091E−08 | 1.855E−06 | 6.166E−01 | 3.339E−06 | 1.362E−01 | 3.984E−02 |
| 0.75 | 5.192E−07 | 2.444E−06 | 6.395E−01 | 2.088E−06 | 1.390E−01 | 4.017E−02 |
| 0.8 | 2.530E−08 | 2.965E−06 | 6.617E−01 | 2.300E−06 | 1.416E−01 | 4.045E−02 |
| 0.85 | 4.328E−07 | 3.364E−06 | 6.833E−01 | 2.684E−06 | 1.443E−01 | 4.068E−02 |
| 0.9 | 2.018E−07 | 2.621E−06 | 7.041E−01 | 2.434E−06 | 1.469E−01 | 4.091E−02 |
| 1 | 7.685E−08 | 3.464E−06 | 7.242E−01 | 4.289E−06 | 1.497E−01 | 4.118E−02 |

**Table 3 Numerical Performance for the LM System-Based $M_i(y)$ Class.**

| $y$ | Min | Med | Max | SIR | STD | Mean |
|---|---|---|---|---|---|---|
| 0 | 8.989E−09 | 3.454E−07 | 1.000E−01 | 4.752E−07 | 1.935E−02 | 5.819E−03 |
| 0.05 | 7.120E−08 | 2.192E−06 | 9.348E−02 | 4.208E−06 | 2.066E−02 | 6.639E−03 |
| 0.1 | 5.372E−07 | 4.453E−06 | 8.783E−02 | 5.981E−06 | 2.115E−02 | 6.757E−03 |
| 0.15 | 3.996E−07 | 4.806E−06 | 8.295E−02 | 7.774E−06 | 2.032E−02 | 6.463E−03 |
| 0.2 | 1.517E−07 | 3.662E−06 | 7.874E−02 | 5.388E−06 | 1.963E−02 | 6.221E−03 |
| 0.25 | 1.200E−07 | 1.933E−06 | 7.513E−02 | 3.386E−06 | 1.903E−02 | 6.021E−03 |
| 0.3 | 7.102E−08 | 9.563E−07 | 7.204E−02 | 1.817E−06 | 1.841E−02 | 5.831E−03 |
| 0.35 | 1.765E−08 | 1.247E−06 | 6.941E−02 | 3.054E−06 | 1.781E−02 | 5.662E−03 |
| 0.4 | 1.604E−07 | 1.952E−06 | 6.719E−02 | 4.035E−06 | 1.728E−02 | 5.524E−03 |
| 0.45 | 9.979E−08 | 2.715E−06 | 6.533E−02 | 4.341E−06 | 1.683E−02 | 5.419E−03 |
| 0.5 | 3.362E−07 | 3.427E−06 | 6.376E−02 | 4.388E−06 | 1.647E−02 | 5.343E−03 |
| 0.55 | 1.489E−07 | 2.954E−06 | 6.247E−02 | 5.733E−06 | 1.617E−02 | 5.293E−03 |
| 0.6 | 6.816E−08 | 3.141E−06 | 6.141E−02 | 5.176E−06 | 1.594E−02 | 5.266E−03 |
| 0.65 | 1.243E−07 | 2.745E−06 | 6.056E−02 | 3.817E−06 | 1.577E−02 | 5.259E−03 |
| 0.7 | 9.518E−08 | 2.019E−06 | 5.988E−02 | 3.339E−06 | 1.565E−02 | 5.269E−03 |
| 0.75 | 4.121E−08 | 1.343E−06 | 5.936E−02 | 2.088E−06 | 1.557E−02 | 5.292E−03 |
| 0.8 | 2.232E−08 | 1.887E−06 | 5.896E−02 | 2.300E−06 | 1.553E−02 | 5.328E−03 |
| 0.85 | 2.691E−09 | 1.268E−06 | 5.867E−02 | 2.684E−06 | 1.552E−02 | 5.372E−03 |
| 0.9 | 1.520E−08 | 2.207E−06 | 5.848E−02 | 2.434E−06 | 1.555E−02 | 5.425E−03 |
| 1 | 1.647E−07 | 2.625E−06 | 5.836E−02 | 4.289E−06 | 1.560E−02 | 5.486E−03 |

to solve the mathematical LM system. It is observed that the proposed MWNNs-AS-GA scheme is accurate, precise and stable.

The GEVAF and GTIC global performances for 30 runs using MWNNs-AS-GA are provided in Table 6 to solve the mathematical LM system. The Min GTIC and GEVAF performances are calculated as $10^{-6} - 10^{-7}, 10^{-10} - 10^{-11}$ and $10^{-8} - 10^{-10}$, whereas the global SIR operator is calculated as $10^{-6} - 10^{-7}, 10^{-10} - 10^{-11}$ and $10^{-7} - 10^{-10}$ to solve the mathematical LM system. The ideal best performances designate the correctness, precision and accurateness of the proposed MWNNs-AS-GA scheme.

**Table 4 Numerical Performance for the LM System-Based $L_r(y)$ Class.**

| $y$ | Min | Med | Max | SIR | STD | Mean |
|---|---|---|---|---|---|---|
| 0 | 7.193E−10 | 4.331E−07 | 1.998E−01 | 4.752E−07 | 4.722E−02 | 1.408E−02 |
| 0.05 | 1.099E−07 | 2.451E−06 | 1.684E−01 | 4.208E−06 | 4.034E−02 | 1.217E−02 |
| 0.1 | 5.599E−08 | 4.007E−06 | 1.667E−01 | 5.981E−06 | 3.507E−02 | 1.042E−02 |
| 0.15 | 5.621E−08 | 3.420E−06 | 1.617E−01 | 7.774E−06 | 3.197E−02 | 8.949E−03 |
| 0.2 | 6.136E−08 | 2.712E−06 | 1.543E−01 | 5.388E−06 | 3.102E−02 | 7.883E−03 |
| 0.25 | 2.300E−08 | 2.028E−06 | 1.451E−01 | 3.386E−06 | 3.129E−02 | 9.353E−03 |
| 0.3 | 3.534E−08 | 1.670E−06 | 1.346E−01 | 1.817E−06 | 3.308E−02 | 1.063E−02 |
| 0.35 | 1.084E−07 | 2.459E−06 | 1.233E−01 | 3.054E−06 | 3.595E−02 | 1.176E−02 |
| 0.4 | 6.087E−08 | 2.175E−06 | 1.555E−01 | 4.035E−06 | 3.949E−02 | 1.279E−02 |
| 0.45 | 1.112E−07 | 2.711E−06 | 1.858E−01 | 4.341E−06 | 4.336E−02 | 1.371E−02 |
| 0.5 | 1.004E−07 | 3.857E−06 | 2.132E−01 | 4.388E−06 | 4.732E−02 | 1.453E−02 |
| 0.55 | 7.858E−08 | 3.178E−06 | 2.380E−01 | 5.733E−06 | 5.119E−02 | 1.525E−02 |
| 0.6 | 4.110E−07 | 3.938E−06 | 2.603E−01 | 5.176E−06 | 5.485E−02 | 1.584E−02 |
| 0.65 | 2.635E−08 | 3.282E−06 | 2.801E−01 | 3.817E−06 | 5.823E−02 | 1.632E−02 |
| 0.7 | 5.219E−08 | 1.604E−06 | 2.975E−01 | 3.339E−06 | 6.131E−02 | 1.666E−02 |
| 0.75 | 6.832E−08 | 2.544E−06 | 3.127E−01 | 2.088E−06 | 6.405E−02 | 1.688E−02 |
| 0.8 | 2.671E−07 | 3.225E−06 | 3.257E−01 | 2.300E−06 | 6.650E−02 | 1.698E−02 |
| 0.85 | 1.424E−07 | 2.925E−06 | 3.367E−01 | 2.684E−06 | 6.850E−02 | 1.758E−02 |
| 0.9 | 1.214E−08 | 2.755E−06 | 3.458E−01 | 2.434E−06 | 7.017E−02 | 1.851E−02 |
| 1 | 1.362E−07 | 3.266E−06 | 3.530E−01 | 4.289E−06 | 7.168E−02 | 1.941E−02 |

**Table 5 Numerical Performance for the LM System-Based $L_i(y)$ Class.**

| $y$ | Min | Med | Max | SIR | STD | Mean |
|---|---|---|---|---|---|---|
| 0 | 1.170E−09 | 1.148E−07 | 1.490E−01 | 6.574E−07 | 3.248E−02 | 1.002E−02 |
| 0.05 | 1.834E−07 | 2.053E−06 | 1.421E−01 | 1.864E−06 | 3.113E−02 | 9.565E−03 |
| 0.1 | 1.882E−07 | 4.026E−06 | 1.352E−01 | 2.762E−06 | 2.983E−02 | 9.141E−03 |
| 0.15 | 3.602E−08 | 4.324E−06 | 1.282E−01 | 2.815E−06 | 2.856E−02 | 8.743E−03 |
| 0.2 | 4.118E−09 | 3.019E−06 | 1.212E−01 | 1.452E−06 | 2.732E−02 | 8.367E−03 |
| 0.25 | 1.146E−07 | 1.405E−06 | 1.142E−01 | 1.389E−06 | 2.612E−02 | 8.012E−03 |
| 0.3 | 6.327E−09 | 1.729E−06 | 1.072E−01 | 1.566E−06 | 2.496E−02 | 7.677E−03 |
| 0.35 | 1.101E−09 | 1.559E−06 | 1.002E−01 | 2.224E−06 | 2.385E−02 | 7.360E−03 |
| 0.4 | 1.113E−07 | 2.892E−06 | 9.326E−02 | 2.395E−06 | 2.278E−02 | 7.062E−03 |
| 0.45 | 1.114E−07 | 3.420E−06 | 8.639E−02 | 2.589E−06 | 2.176E−02 | 6.780E−03 |
| 0.5 | 3.764E−08 | 3.247E−06 | 8.291E−02 | 2.880E−06 | 2.080E−02 | 6.513E−03 |
| 0.55 | 1.596E−07 | 3.404E−06 | 8.213E−02 | 2.541E−06 | 1.991E−02 | 6.262E−03 |
| 0.6 | 1.476E−07 | 3.095E−06 | 8.148E−02 | 2.240E−06 | 1.908E−02 | 6.026E−03 |
| 0.65 | 1.773E−07 | 1.757E−06 | 8.096E−02 | 2.093E−06 | 1.832E−02 | 5.805E−03 |
| 0.7 | 6.341E−09 | 1.309E−06 | 8.057E−02 | 1.851E−06 | 1.765E−02 | 5.599E−03 |
| 0.75 | 1.126E−08 | 1.859E−06 | 8.029E−02 | 2.563E−06 | 1.706E−02 | 5.408E−03 |
| 0.8 | 1.022E−07 | 1.396E−06 | 8.013E−02 | 2.408E−06 | 1.657E−02 | 5.230E−03 |
| 0.85 | 1.412E−08 | 1.355E−06 | 8.008E−02 | 1.891E−06 | 1.618E−02 | 5.065E−03 |
| 0.9 | 4.870E−08 | 1.698E−06 | 8.013E−02 | 1.405E−06 | 1.589E−02 | 4.911E−03 |
| 1 | 4.591E−08 | 2.608E−06 | 8.215E−02 | 2.298E−06 | 1.601E−02 | 4.828E−03 |

**Table 6 Global MAD, TIC and EVAF Performances for the Mathematical LM System.**

| | GMAD | | GTIC | | GTIC | |
|---|---|---|---|---|---|---|
| Index | Min | SIR | Min | SIR | Min | SIR |
| $M_r(y)$ | 4.27E−06 | 4.49E−06 | 2.36E−10 | 2.29E−10 | 3.21E−10 | 4.94E−10 |
| $M_i(y)$ | 2.41E−06 | 1.70E−06 | 1.32E−10 | 8.40E−11 | 1.80E−08 | 2.28E−08 |
| $L_r(y)$ | 2.67E−06 | 3.93E−06 | 1.51E−10 | 1.96E−10 | 1.16E−10 | 3.36E−10 |
| $L_i(y)$ | 2.75E−06 | 1.24E−06 | 1.52E−10 | 7.46E−11 | 7.27E−08 | 1.00E−07 |

## 6. CONCLUSIONS

The design of this study is to design a novel stochastic solver through the Morlet wavelet neural networks for solving the mathematical Layla and Majnun model. The numerical representations of the mathematical LM system have been presented through the MWNNs along with the optimization procedures of the global and local search schemes. The local active-set and global genetic algorithm operators have been used to optimize an error-based merit function using the differential LM model and its initial conditions. To perform the exactness of the mathematical LM system, the comparison of the proposed and reference results is presented through the hybridization of AS-GA scheme. In order to observe the precision and accuracy of the MWNNs-AS-GA, the EVAF and TIC along with the MAD performances are provided for thirty executions using 120 variables or 10 neurons. The EVAF and TIC operators have been obtained in reliable measures to solve each class of the mathematical LM model. The valuations through Min, Med, Max, S.I.R, SD and Mean measures verify the significance of the proposed MWNNs-AS-GA scheme. The global values are obtained through statistical measures to solve the mathematical LM system.

The MWNN-AS-GA is applied in future to solve the fluidics, biological, prediction and other potential nonlinear systems.[61–68]

## REFERENCES


1. G. Baghdadi, S. Jafari, J. C. Sprott, F. Towhidkhah and M. H. Golpayegani, A chaotic model of sustaining attention problem in attention deficit disorder, *Commun. Nonlinear Sci. Numer. Simul.* **20**(1) (2015) 174–185.
2. J. C. Sprott, Dynamical models of happiness, *Nonlinear Dyn. Psychol. Life Sci.* **9**(1) (2005) 23–36.
3. S. Jafari, Z. Ansari, S. M. R. H. Golpayegani and S. Gharibzadeh, Is attention a "period window" in the chaotic brain? *J. Neuropsychiatry Clin. Neurosci.* **25**(1) (2013) E05.
4. S. S. Tabatabaei, M. J. Yazdanpanah, S. Jafari and J. C. Sprott, Extensions in dynamic models of happiness: Effect of memory, *Int. J. Happiness Dev.* **1**(4) (2014) 344–356.
5. X. Liao and J. Ran, Hopf bifurcation in love dynamical models with nonlinear couples and time delays, *Chaos Solitons Fractals* **31**(4) (2007) 853–865.
6. F. Dercole and S. Rinaldi, Love stories can be unpredictable: Jules et Jim in the vortex of life, *Chaos* **24**(2) (2014) 023134.
7. F. Breitenecker, F. Judex, N. Popper, K. Breitenecker, A. Mathe and A. Mathe, Love emotions between laura and petrarchan approach by mathematics and system dynamics, *J. Comput. Inf. Technol.* **16**(4) (2008) 255–269.
8. V. A. Rozhansky and L. D. Tsendin, *Transport Phenomena in Partially Ionized Plasma* (CRC Press, 2001).
9. R. Alves-Pires, *Nonlinear Dynamics in Particle Accelerators*, Vol. 23 (World Scientific, 1996).
10. A. Newell and J. Moloney, *Nonlinear Optics* (Addison-Wesley, Reading, Massachusetts, 1992).
11. L. Cveticanin, Resonant vibrations of nonlinear rotors, *Mech. Mach. Theory* **30**(4) (1995) 581–588.
12. M. Farman, A. Akgül, S. F. Aldosary, K. S. Nisar and A. Ahmad, Fractional order model for complex Layla and Majnun love story with chaotic behaviour, *Alexandria Eng. J.* **61**(9) (2022) 6725–6738.
13. Z. Sabir, M. Umar, M. A. Z. Raja, H. M. Baskonus and W. Gao, Designing of Morlet wavelet as a neural network for a novel prevention category in the HIV system, *Int. J. Biomath.* **15**(04) (2022) 2250012.
14. S. Ahmad, A. Ullah, A. Akgül and D. Baleanu, Theoretical and numerical analysis of fractal fractional model of tumor-immune interaction with two different kernels, *Alexandria Eng. J.* **61**(7) (2022) 5735–5752.
15. L. Xuan, S. Ahmad, A. Ullah, S. Saifullah, A. Akgül and H. Qu, Bifurcations, stability analysis and complex dynamics of Caputo fractal-fractional cancer model, *Chaos Solitons Fractals* **159** (2022) 112113.
16. R. Safdar, M. Jawad, S. Hussain, M. Imran, A. Akgül and W. Jamshed, Thermal radiative mixed convection flow of MHD Maxwell nanofluid: Implementation of Buongiorno's model, *Chin. J. Phys.* **77** (2022) 1465–1478.
17. A. Akgül and M. Partohaghighi, New fractional modelling and control analysis of the circumscribed self-excited spherical strange attractor, *Chaos Solitons Fractals* **158** (2022) 111956.
18. X. Liu, S. Ahmad, M. ur Rahman, Y. Nadeem and A. Akgül, Analysis of a TB and HIV co-infection model under Mittag-Leffler fractal-fractional derivative, *Phys. Scr.* **97**(5) (2022) 054011.
19. E. F. D. Goufo, C. Ravichandran and G. A. Birajdar, Self-similarity techniques for chaotic attractors with many scrolls using step series switching, *Math. Model. Anal.* **26**(4) (2021) 591–611.
20. K. Logeswari, C. Ravichandran and K. S. Nisar, Mathematical model for spreading of COVID-19 virus with the Mittag–Leffler kernel, *Numerical*

*Methods for Partial Differential Equations* (2020), doi:10.1002/num.22652.
21. K. S. Nisar, K. Logeswari, V. Vijayaraj, H. M. Baskonus and C. Ravichandran, Fractional order modeling the Gemini Virus in capsicum annuum with optimal control, *Fractal Fract.* **6**(2) (2022) 61.
22. T. A. Jumani, M. W. Mustafa, Z. Hussain, M. M. Rasid, M. S. Saeed, M. M. Memon, I. Khan and K. S. Nisar, Jaya optimization algorithm for transient response and stability enhancement of a fractional-order PID based automatic voltage regulator system, *Alexandria Eng. J.* **59**(4) (2020) 2429–2440.
23. G. Rahman, Z. Ullah, A. Khan, E. Set and K. S. Nisar, Certain Chebyshev-type inequalities involving fractional conformable integral operators, *Mathematics* **7**(4) (2019) 364.
24. M. Farman, A. Ahmad, A. Akgül, M. U. Saleem, K. S. Nisar and V. Vijayakumar, Dynamical behavior of tumor-immune system with fractal-fractional operator, *AIMS Math.* **7**(5) (2022) 8751–8773.
25. S. W. Yao, M. Farman, M. Amin, M. Inc, A. Akgül and A. Ahmad, Fractional order COVID 19 model with transmission rout infected through environment, *AIMS Math.* **7**(4) (2022) 51565174.
26. M. Farman, A. Akgül, M. T. Tekin, M. M. Akram, A. Ahmad, E. E. Mahmoud and I. S. Yahia, Fractal fractional-order derivative for HIV/AIDS model with Mittag-Leffler kernel, *Alexandria Eng. J.* **61**(12) (2022) 10965–10980.
27. M. Farman, M. Aslam, A. Akgül and F. Jarad, On solutions of the stiff differential equations in chemistry kinetics with fractal-fractional derivatives, *J. Comput. Nonlinear Dyn.* **17**(7) (2022) 071007.
28. L. Cveticanin, Approximate analytical solutions to a class of non-linear equations with complex functions, *J. Sound Vib.* **157**(2) (1992) 289–302.
29. G. M. Mahmoud and S. A. Aly, On periodic solutions of parametrically excited complex non-linear dynamical systems, *Physica A* **278**(3–4) (2000) 390–404.
30. X. Wu, Y. Xu and H. Zhang, Random impacts of a complex damped system, *Int. J. Non-Linear Mech.* **46**(5) (2011) 800–806.
31. S. E. Awan *et al.*, Numerical treatments to analyze the nonlinear radiative heat transfer in MHD nanofluid flow with solar energy, *Arabian J. Sci. Eng.* **45**(6) (2020) 4975–4994.
32. S. E. Awan *et al.*, Numerical computing paradigm for investigation of micropolar nanofluid flow between parallel plates system with impact of electrical MHD and Hall current, *Arabian J. Sci. Eng.* **46**(1) (2021) 645–662.
33. M. Shoaib *et al.*, Numerical investigation for rotating flow of MHD hybrid nanofluid with thermal radiation over a stretching sheet, *Sci. Rep.* **10**(1) (2020) 1–15.
34. S. Jafari, J. C. Sprott and S. M. R. H. Golpayegani, Layla and Majnun: A complex love story, *Nonlinear Dyn.* **83**(1) (2016) 615–622.
35. P. Kumar, V. S. Erturk and M. Murillo-Arcila, A complex fractional mathematical modeling for the love story of Layla and Majnun, *Chaos Solitons Fractals* **150** (2021) 111091.
36. Z. Sabir, M. A. Z. Raja, J. L. Guirao and T. Saeed, Swarm intelligence procedures using Meyer wavelets as a neural network for the novel fractional order pantograph singular system, *Fractal Fract.* **5**(4) (2021) 277.
37. P. Junsawang, S. Zuhra, Z. Sabir, M. A. Z. Raja, M. Shoaib, T. Botmart and W. Weera, Numerical simulations of vaccination and Wolbachia on dengue transmission dynamics in the nonlinear model, *IEEE Access* **10** (2022) 31116–31144.
38. M. A. Z. Raja, M. Shoaib, S. Hussain, K. S. Nisar and S. Islam, Computational intelligence of Levenberg-Marquardt backpropagation neural networks to study thermal radiation and Hall effects on boundary layer flow past a stretching sheet, *Int. Commun. Heat Mass Transfer* **130** (2022) 105799.
39. Z. Sabir *et al.*, Numerical investigations of the nonlinear smoke model using the Gudermannian neural networks, *Math. Biosci. Eng.* **19**(1) (2022) 351–370.
40. Z. Sabir *et al.*, An efficient stochastic numerical computing framework for the nonlinear higher order singular models, *Fractal Fract.* **5**(4) (2021) 176.
41. Z. Sabir *et al.*, Design of Morlet wavelet neural network for solving the higher order singular nonlinear differential equations, *Alexandria Eng. J.* **60**(6) (2021) 5935–5947.
42. M. Umar *et al.*, A stochastic intelligent computing with neuro-evolution heuristics for nonlinear SITR system of novel COVID-19 dynamics, *Symmetry* **12**(10) (2020) 1628.
43. M. Umar *et al.*, Integrated neuro-swarm heuristic with interior-point for nonlinear SITR model for dynamics of novel COVID-19, *Alexandria Eng. J.* **60**(3) (2021) 2811–2824.
44. M. Umar *et al.*, Neuro-swarm intelligent computing paradigm for nonlinear HIV infection model with CD4+ T-cells, *Math. Comput. Simul.* **188** (2021) 241–253.
45. M. Umar *et al.*, A novel study of Morlet neural networks to solve the nonlinear HIV infection system of latently infected cells, *Results Phys.* **25** (2021) 104235.
46. M. Shoaib *et al.*, Heat transfer impacts on Maxwell nanofluid flow over a vertical moving surface with MHD using stochastic numerical technique via artificial neural networks, *Coatings* **11**(12) (2021) 1483.

47. M. Shoaib *et al.*, Intelligent computing with LevenbergMarquardt backpropagation neural networks for third-grade nanofluid over a stretched sheet with convective conditions, *Arabian J. Sci. Eng.* **47** (2022) 8211–8229.
48. Z. Sabir *et al.*, A neuro-swarming intelligence-based computing for second order singular periodic nonlinear boundary value problems, *Front. Phys.* **8** (2020) 224.
49. M. Umar *et al.*, A stochastic numerical computing heuristic of SIR nonlinear model based on dengue fever, *Results Phys.* **19** (2020) 103585.
50. Z. Sabir, J. L. Guirao and T. Saeed, Solving a novel designed second order nonlinear Lane–Emden delay differential model using the heuristic techniques, *Appl. Soft Comput.* **102** (2021) 107105.
51. Z. Tao, L. Huiling, W. Wenwen and Y. Xia, GA-SVM based feature selection and parameter optimization in hospitalization expense modeling, *Appl. Soft Comput.* **75** (2019) 323–332.
52. Z. Sabir, M. A. Manzar, M. A. Z. Raja, M. Sheraz and A. M. Wazwaz, Neuro-heuristics for nonlinear singular Thomas-Fermi systems, *Appl. Soft Comput.* **65** (2018) 152–169.
53. M. Ilbeigi, M. Ghomeishi and A. Dehghanbanadaki, Prediction and optimization of energy consumption in an office building using artificial neural network and a genetic algorithm, *Sustain. Cities Soc.* **61** (2020) 102325.
54. F. Altaf *et al.*, Adaptive evolutionary computation for nonlinear Hammerstein control autoregressive systems with key term separation principle, *Mathematics* **10**(6) (2022) 1001.
55. A. Mehmood *et al.*, Integrated computational intelligent paradigm for nonlinear electric circuit models using neural networks, genetic algorithms and sequential quadratic programming, *Neural Comput. Appl.* **32**(14) (2020) 10337–10357.
56. Z. Sabir, C. M. Khalique, M. A. Z. Raja and D. Baleanu, Evolutionary computing for nonlinear singular boundary value problems using neural network, genetic algorithm and active-set algorithm, *Eur. Phys. J. Plus* **136**(2) (2021) 1–19.
57. Z. Sabir, Stochastic numerical investigations for nonlinear three-species food chain system, *Int. J. Biomath.* **15**(4) (2022) 2250005.
58. X. He and P. Yang, The primal-dual active set method for a class of nonlinear problems with T-monotone operators, *Math. Probl. Eng.* **2019** (2019) 2912301.
59. M. A. Z. Raja, M. Umar, Z. Sabir, J. A. Khan and D. Baleanu, A new stochastic computing paradigm for the dynamics of nonlinear singular heat conduction model of the human head, *Eur. Phys. J. Plus* **133**(9) (2018) 1–21.
60. M. Umar, M. A. Z. Raja, Z. Sabir, A. S. Alwabli and M. Shoaib, A stochastic computational intelligent solver for numerical treatment of mosquito dispersal model in a heterogeneous environment, *Eur. Phys. J. Plus* **135**(7) (2020) 1–23.
61. S. Naz *et al.*, Neuro-intelligent networks for BoucWen hysteresis model for piezostage actuator, *Eur. Phys. J. Plus* **136**(4) (2021) 1–20.
62. Z. Sabir, M. A. Z. Raja and D. Baleanu, Fractional mayer neuro-swarm heuristic solver for multi-fractional order doubly singular model based on Lane–Emden equation, *Fractals* **29**(5) (2021) 2140017.
63. Z. Sabir, D. Baleanu, M. A. Z. Raja and J. L. Guirao, Design of neuro-swarming heuristic solver for multi-pantograph singular delay differential equation, *Fractals* **29**(5) (2021) 2140022.
64. A. H. Bukhari *et al.*, Design of intelligent computing networks for nonlinear chaotic fractional Rossler system, *Chaos Solitons Fractals* **157** (2022) 111985.
65. A. K. Kiani, W. U. Khan, M. A. Z. Raja, Y. He, Z. Sabir and M. Shoaib, Intelligent backpropagation networks with bayesian regularization for mathematical models of environmental economic systems, *Sustainability* **13**(17) (2021) 9537.
66. B. Wang *et al.*, Numerical computing to solve the nonlinear corneal system of eye surgery using the capability of Morlet wavelet artificial neural networks, *Fractals* **30** (2022) 2240147.
67. B. Wang *et al.*, Gudermannian neural networks to investigate the Lienard differential model, *Fractals* **30** (2022) 2250050.
68. Z. Sabir, M. A. Z. Raja, J. L. Guirao and T. Saeed, Meyer wavelet neural networks to solve a novel design of fractional order pantograph Lane-Emden differential model, *Chaos Solitons Fractals* **152** (2021) 111404.